



Cylindrical convergence effects on the Rayleigh-Taylor instability in elastic and viscous mediaA. R. Piriz **Instituto de Investigaciones Energéticas (INEI), E.T.S.I.A., and CYTEMA, Universidad de Castilla-La Mancha, 13071 Ciudad Real, Spain*S. A. Piriz *Instituto de Investigaciones Energéticas (INEI), E.T.S.I.A., and CYTEMA, Universidad de Castilla-La Mancha, 45071 Toledo, Spain*

N. A. Tahir

GSI Helmholtzzentrum für Schwerionenforschung Darmstadt, Planckstrasse 1, 64291 Darmstadt, Germany

(Received 19 March 2022; accepted 30 June 2022; published 22 July 2022)

Convergence effects on the perturbation growth of an imploding surface separating two nonideal material media (elastic and viscous media) are analyzed in the case of a cylindrical implosion in both the Rayleigh-Taylor stable and unstable configurations. In the stable configuration, the perturbation damping effect due to angular momentum conservation becomes destroyed for sufficiently high values of the elastic modulus or of the viscosity of the media. For the unstable configuration, Rayleigh-Taylor instability can be suppressed by the elasticity or mitigated by the viscosity, but without practically affecting the perturbation growth due to the geometrical convergence. However, the convergence effects manifest themselves in a manner somewhat different from the classical Bell-Plesset effect by making the process more sensitive to the media compressibility than in the case involving ideal media.

DOI: [10.1103/PhysRevE.106.015109](https://doi.org/10.1103/PhysRevE.106.015109)**I. INTRODUCTION**

It is already a well established fact that the effect of geometrical convergence, known as the Bell-Plesset (BP) effect, on the growth of perturbations in an accelerated cylindrical or spherical surface, influences the evolution of the Rayleigh-Taylor instability (RTI) [1–10].

The basic case is the one present in the implosion of cavities or single interfaces involving two ideal fluids, although a few works have also considered finite thickness shells in which the convergence effects arise on both surfaces [3,4,8]. More recently, the presence of viscosity was also included in the analysis of an expanding cavity, but a specific study of the viscous effects was not further considered [11]. On the other hand, several studies involving ideal media have shown that BP effects are mitigated by the compressibility of the media, although in some situations complete suppression may require somewhat unrealistic levels of compressibility [5–7].

Except for the few works mentioned above, BP effects have been mostly studied on single interfaces representing either the outer or the inner surface of a shell, which is quite appropriate for relatively thick shells in which feedthrough effects can be ignored or at least separated from the growth of the perturbations due to the geometrical convergence, or from the RT evolution on the surface itself without feeding from the other one.

In addition, the different phases of an implosion, which include an acceleration stage followed by a stagnation phase,

have been usually treated together, thus making it difficult to discriminate the different response of the interface in each regime. However, the convergence ratio C_2 during the stagnation phase is in general not very large, and, as will be shown, the contribution of this stage to the perturbations growth due the geometrical effects is much less significant than the growth due to the RTI. In fact, it was already shown by Book and Bodner that in spherical implosions it is $C_2 \sim 2$ [3]. Furthermore, if compressibility effects are going to be of relevance, it should be expected that such effects would be stronger just on this late phase. Therefore, the perturbation growth during the stagnation phase can be satisfactorily studied by neglecting BP effects and analyzing RTI under conditions in which the curvature effects are relevant [12–15]. Then, it seems reasonable to restrict the analysis of the convergence effects during the implosion to the phase of inward acceleration. This is the approach we have adopted for the analysis of the LAPLAS (Laboratory Planetary Science) experimental setup that is being designed in the framework of the international collaboration on high-energy density physics at the Facility for Antiproton and Ion Research (FAIR) presently in the final phase of construction at the GSI Helmholtzzentrum Darmstadt (Germany) [16–26,28].

The LAPLAS experiment consists in a cylindrical shell (the payload) containing a material sample in the interior that is imploded by using an intense beam of heavy ions with an annular focal spot (Fig. 1). The beam impinges axially and heats the annular region (the absorber) surrounding the payload, which expands and accelerates the pusher radially inward, thus compressing the sample [25–27]. The external

*roberto.piriz@uclm.es

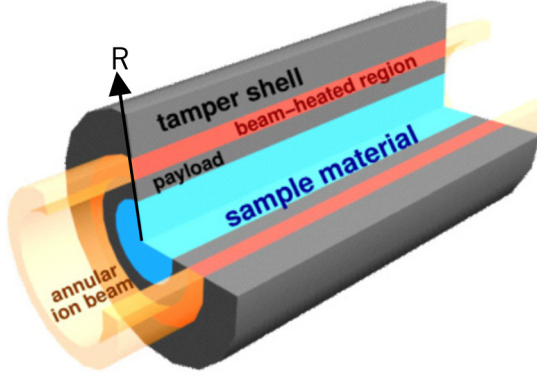


FIG. 1. Schematic of the LAPLAS experiment.

shell (the tamper) avoids the outward expansion of the absorber optimizing the efficiency of the implosion process. The high-density payload material, namely tungsten, ensures a quasi-isentropic compression of the sample, but it also makes the acceleration process potentially susceptible to Rayleigh-Taylor instability. For this, LAPLAS relies on the mechanical properties of the pusher material to provide the stabilizing mechanism that would safeguard the implosion process from the deleterious effects of the hydrodynamic instabilities [29–40]. In addition, both the inner and outer surfaces of the shell may be affected by the geometrical convergence or BP effects that could further enhance the amplitude of the perturbations.

Although the convergence ratio of the pusher in LAPLAS is not very large ($C_e = R_{e0}/R_{em} \approx 1.5$ for the external surface and $C_i = R_0/R_{im} \leq 3.5$ for the internal surface, where R_{e0} and R_0 are, respectively, the initial radii of the external and internal surfaces; and R_{em} and R_{im} are the respective minimum radii during the implosion), the influence of the mechanical properties of the pusher on the geometrical convergence effects needs to be evaluated in order to learn about the possible synergetic among such mechanical properties of the material, the convergence process, and compressibility.

For this, in this work we study the BP effects on a single interface, taking into account the compressibility of the pusher and the elasticity of the medium, because a stable elastic phase is a necessary condition for the RT stability of an elastic-plastic medium [32,38]. The presence of viscosity will also be considered. We restrict ourselves to the implosion phase, and we consider separately the situations that suitably describe the behavior of the external and internal surfaces of the pusher, ignoring the feedthrough process (thick shell approximation).

II. FUNDAMENTAL EQUATIONS

We consider an imploding cylindrical surface of radius $R = R(t)$ that separates two media of uniform densities ρ_1 ($r \leq R$) and ρ_2 ($r \geq R$). To keep the problem tractable, the media are considered to develop irrotational fields of velocity and displacements, both for the background flow and for the perturbations, so that these fields are determined from scalar potentials. The nonideal effects could be introduced to zero order as boundary conditions in the same manner as was done to consider the viscosity effects in the dynamics of bubbles

[41]. However, as we can see below, such effects are not going to alter the velocity profiles, and therefore they will not directly alter the dynamics of the interface implosion.

Then, the flow can be described by the following equations for mass and momentum conservation:

$$\frac{d\rho_n}{dt} + \rho_n \vec{\nabla} \cdot \vec{v}_n = 0, \quad (1)$$

$$\rho_n \frac{d\vec{v}_n}{dt} = -\vec{\nabla} p_n, \quad (2)$$

where $n = 1, 2$ denotes the internal and the external medium, respectively, \vec{v}_n and p_n are the flow velocity and the pressure of the medium n , respectively, and the material derivative of any magnitude M is

$$\frac{dM}{dt} = \frac{\partial M}{\partial t} + \vec{v}_n \cdot \vec{\nabla} M = 0. \quad (3)$$

In addition, the assumption of an irrotational velocity field allowed us to define the velocity potential:

$$\vec{\nabla} \phi_n = \vec{v}_n. \quad (4)$$

Therefore, we will consider first the dynamics of the background flow.

A. Background dynamics

As in previous studies, we assume that densities ρ_n are uniform, so that Eq. (1) can be integrated to obtain the following expression for the radial velocity in the medium n :

$$v_n = \frac{R\dot{R}}{r} \left(1 - \frac{\alpha_n}{2}\right) + \frac{\alpha_n \dot{R}}{2R} r, \quad (5)$$

where we have defined α_n such that

$$\frac{\dot{\rho}_n}{\rho_n} = -\alpha_n \frac{\dot{R}}{R}, \quad (6)$$

and an overdot indicates time derivative.

In particular, by substituting Eq. (5) into Eq. (2), we obtain

$$\begin{aligned} & \left(1 - \frac{\alpha_2}{2}\right) (\ddot{R}R + \dot{R}^2) \frac{1}{r} + \frac{\alpha_2}{2} \left[\frac{\ddot{R}}{R} - \left(1 - \frac{\alpha_2}{2}\right) \frac{\dot{R}^2}{R^2} \right] r \\ & - \left(1 - \frac{\alpha_2}{2}\right)^2 \frac{\dot{R}^2 R^2}{r^3} = -\frac{1}{\rho_2} \frac{dp_2}{dr}. \end{aligned} \quad (7)$$

As is well known, is not possible to integrate this equation up to an external radius $R_e \rightarrow \infty$ to get the evolution equation for a cavity of radius R . However, as was shown in Refs. [42,43], in considering a suitably thick shell or a cavity, a reasonable approximation is to integrate up a radius $R_e \sim 10R$, where an external pressure p_e is applied. Here, we will assume a thick shell with a given constant mass m_2 , and then the external radius R_e will be determined by the mass conservation:

$$\frac{R_e}{R} = \left(1 + \frac{m_2}{\pi \rho_2 R^2}\right)^{1/2}, \quad \frac{\rho_2}{\rho_{20}} = \left(\frac{R_0}{R}\right)^{\alpha_2}, \quad (8)$$

where ρ_{20} is the initial density of the medium “2,” and we remind the reader that R_0 is the initial radius of the internal surface of the shell. The second part of the previous

equation comes from the integration of Eq. (6). Then, upon integration of Eq. (7), it turns out that

$$\begin{aligned} \frac{p_1 - p_e}{\rho_2} &= \left(1 - \frac{\alpha_2}{2}\right) (\ddot{R}R) + \dot{R}^2 \ln \frac{R_e}{R} \\ &+ \frac{\alpha_2}{4} \left[\frac{\ddot{R}}{R} - \left(1 - \frac{\alpha_2}{2}\right) \frac{\dot{R}^2}{R^2} \right] (R_e^2 - R^2) \\ &+ \left(1 - \frac{\alpha_2}{2}\right)^2 \frac{\dot{R}^2 R^2}{2} \left(\frac{1}{R_e^2} - \frac{1}{R^2} \right), \end{aligned} \quad (9)$$

where p_1 is the pressure in the internal region. The previous equation must be solved with the following initial conditions:

$$R(0) = R_0, \quad \dot{R}(0) = 0. \quad (10)$$

Introducing the following dimensionless magnitudes:

$$x = \frac{R}{R_0}, \quad T = \frac{t}{t_0}, \quad (11)$$

and after rearranging the terms, Eq. (9) reads

$$\begin{aligned} &2x^{\alpha_2} (\Pi_0 x^{-\alpha_1 \gamma} - 1) \\ &= \ddot{x} x \left[\left(1 - \frac{\alpha_2}{2}\right) \ln(1 + a_0 x^{\alpha_2 - 2}) + a_0 \frac{\alpha_2}{2} x^{\alpha_2 - 2} \right] \\ &+ \left(1 - \frac{\alpha_2}{2}\right) \dot{x}^2 \left[\ln(1 + a_0 x^{\alpha_2 - 2}) - \frac{2 + \alpha_2 a_0 x^{\alpha_2 - 2}}{1 + a_0 x^{\alpha_2 - 2}} \frac{a_0}{2} x^{\alpha_2 - 2} \right], \end{aligned} \quad (12)$$

and the initial conditions read

$$x(0) = 1, \quad \dot{x}(0) = 0. \quad (13)$$

In writing Eq. (12), we have considered that the internal medium is compressed adiabatically with an adiabatic index γ [8], so that

$$p_1 = p_0 \left(\frac{\rho_1}{\rho_{10}} \right)^\gamma = \left(\frac{R_0}{R} \right)^{\alpha_1 \gamma}, \quad (14)$$

and, for writing Eq. (14), we have integrated Eq. (6) for the medium “1.” If the mass of the internal medium is conserved, then it turns out $\alpha_1 = 2$. If not, it must be assumed that a convenient sink of mass exists in the internal region in order to allow for an arbitrary value of α_1 [5–8].

In addition, in Eq. (12) we set

$$\Pi_0 = \frac{p_0}{p_e}, \quad t_0 = \sqrt{\frac{\rho_2 R_0^2}{p_e}}, \quad a_0 = \frac{m_2}{\pi R_0^2 \rho_{20}}, \quad (15)$$

where the parameter a_0 accounts for the thickness of the shell.

To study the convergence effects on the growth of the perturbation amplitude, we are particularly interested in the situations with $\Pi_0 \ll 1$ for which we have the maximum convergence ratio.

In Fig. 2 we have represented a typical solution of Eq. (12) for $\Pi_0 = 0.05$, a not too small value so that the scale of the stagnation phase remains reasonably appreciable. Figure 2(a) shows the interface trajectory $R(t)$, the velocity $\dot{R}(t)$, and the acceleration $\ddot{R}(t)$. Figure 2(b) shows a detailed view of the slowing-down phase, starting at the time T_1 (when the imploding velocity is maximum), in which we can see that the convergence ratio $C_2 = R(T_1)/R(T_2)$ is not very significant

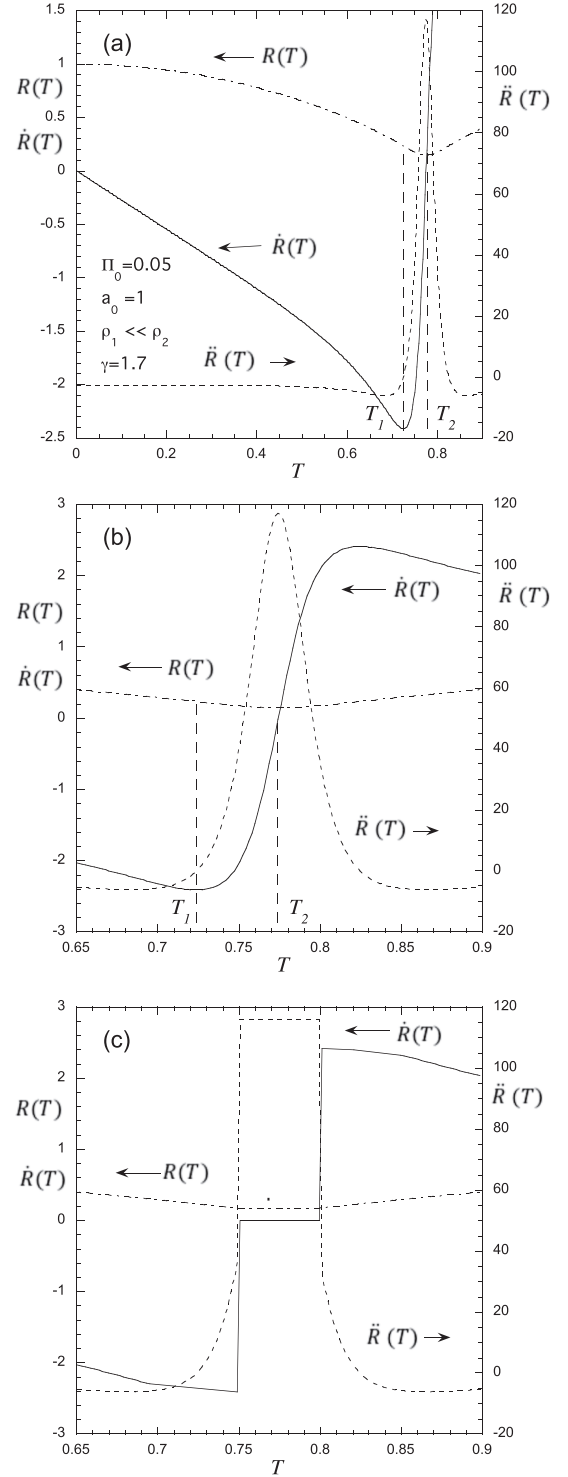


FIG. 2. (a) Time evolution of the radius $R(t)$, velocity $\dot{R}(t)$, and acceleration $\ddot{R}(t)$ of the shell internal surface; (b) detail of $R(t)$, $\dot{R}(t)$, and $\ddot{R}(t)$ during the stagnation phase; (c) idealization of the stagnation phase evolution. Arrows indicate the corresponding axes.

(T_2 is the time when the minimum radius is achieved). This fact is shown more clearly in Table I, where the convergence ratios $C_1 = R_0/R(T_1)$ and C_2 are given for a wide range of variation of the parameters Π_0 and a_0 , and for $\rho_1 \ll \rho_2$. As can be noticed, the convergence ratio C_2 during the stagnation

TABLE I. Convergence ratios during the acceleration phase C_1 and during the stagnation phase C_2 for different dimensionless driving pressures Π_0 and shell thicknesses a_0 , and $\gamma = 1.7$.

	$\Pi_0 = 0.1$	$\Pi_0 = 001$	$\Pi_0 = 0.001$
$a_0(R_0/\Delta)$	$C_1 C_2$	$C_1 C_2$	$C_1 C_2$
1.00 (2.40)	2.70 1.59	13.50 1.58	67.50 1.63
0.10 (20.4)	2.10 2.01	12.70 1.66	59.10 1.94
0.05 (40.5)	2.03 2.10	12.30 1.69	53.10 2.02

phase is practically constant and it is $C_2 \approx 1.6$ to 2, so that the convergence effects on the perturbation growth in this phase cannot be very important, and it can be reasonably assumed that such a phase is dominated by the RTI with, of course, the curvature effects taken into account [15]. This conclusion is reinforced by the influence of the compressibility on the convergence effects [4–7], which is expected to be the maximum just during the stagnation phase. A similar conclusion was obtained by Book and Bodner in their analysis of the convergence effects in a spherical implosion [3].

Therefore, the situation at the stagnation can be idealized as shown in Fig. 2(c). Such an approach has, in fact, been adopted in several studies of the RTI spherical and cylindrical interfaces [12–14,44], and it seems to be well supported by the implosion dynamics.

Therefore, in the following, we can limit our analysis of the convergence effects to the phase of inward acceleration of the cavity.

B. Linear analysis

As a first step, we revisit the case involving ideal fluids considered in Refs. [4–7] in order to find the equation for the perturbation evolution in cylindrical geometry including the compressibility of the background flow but assuming incompressible perturbations.

1. Ideal media

We linearize Eqs. (1) and (2) in the usual manner by writing every magnitude M (i.e., \vec{v} , ρ , and p) as $M = M_0 + \delta M$, where M_0 and $\delta M \ll M_0$ are the background value and its perturbation, respectively. Thus, we obtain [15]

$$\vec{\nabla} \cdot (\delta \vec{v}_n) = 0, \quad (16)$$

$$\rho_n \frac{\partial^2 \phi_n}{\partial t^2} + \delta p_n + \rho_n \ddot{R} \eta_{rn} = 0, \quad (17)$$

where $\delta \vec{v}_n = \vec{\nabla}(\delta \phi_n)$, and η_{rn} is the radial component of the displacement $\vec{\eta}(\theta, t)$ with respect to the interface ($\vec{\eta} = \delta \vec{v}_n$, and θ is the azimuthal coordinate).

Then, from Eq. (13) and considering that $\delta \phi_2 \rightarrow 0$ for $r \rightarrow \infty$, and that $\delta \phi_1$ must be finite at $r = 0$, we obtain

$$\delta \phi_2 = \frac{a_2}{r^m} \cos m\theta, \quad (18)$$

$$\delta \phi_1 = a_1 r^m \cos m\theta, \quad (19)$$

where a_1 and a_2 are constants to be determined from the boundary conditions, and $m = kr$ is the perturbation mode ($k = 2\pi/\lambda$, and λ is the perturbation wavelength).

The boundary conditions at $r = R$ are given by the continuity of the velocity and of the normal stress:

$$\dot{\eta}_{r1}(R) = \dot{\eta}_{r2}(R) = \dot{\xi}(t) \cos m\theta, \quad (20)$$

$$\delta p_1(R) = \delta p_2(R), \quad (21)$$

where $\xi(t)$ is the perturbation amplitude, δp_n is given by Eq. (17), and

$$\dot{\eta}_{rn}(R) = v_n(R + \eta) - \dot{R} = \delta v_n + \frac{\partial v_n}{\partial r} \Big|_{r=R}, \quad (22)$$

$$\delta v_n = \delta v_n(R) = \frac{\partial(\delta \phi_n)}{\partial r} \Big|_{r=R}. \quad (23)$$

By using Eq. (5) in the velocity derivative of Eq. (22), we obtain

$$\delta v_n = \dot{\eta}_{rn} - (\alpha_n - 1) \eta_{rn} \frac{\dot{R}}{R}, \quad (24)$$

which, together with Eqs. (18), (19), and (23), yields the following relationships for determining a_1 and a_2 :

$$\dot{\xi} = -\frac{ma_2}{R^{m+1}} + (\alpha_2 - 1) \xi \frac{\dot{R}}{R}, \quad (25)$$

$$\dot{\xi} = -ma_1 R^{m-1} + (\alpha_1 - 1) \xi \frac{\dot{R}}{R}. \quad (26)$$

Therefore, from the boundary condition equations and taking, for simplicity, α_n as constants, we obtain the following equation for the perturbation evolution:

$$\ddot{\xi} + \frac{(2 - \alpha_2)\rho_2 + (2 - \alpha_1)\rho_1}{\rho_2 + \rho_1} \xi \frac{\dot{R}}{R} - \frac{(m + \alpha_2 - 1)\rho_2 - (m - \alpha_1 + 1)\rho_1}{\rho_2 + \rho_1} \xi \frac{\ddot{R}}{R} = 0. \quad (27)$$

This is the cylindrical version of the equation obtained by Ramshaw and Amendt [6] in spherical geometry, for the particular case of constant values for α_n . However, the extension to $\alpha_n = \alpha_n(t)$ is straightforward and it is not necessary for our present purposes. Of course, when the mass of the interior medium is conserved it turns out to be $\alpha_1 = 2$, and for an incompressible external medium it is $\alpha_2 = 0$. This particular choice of values is suitable for describing the perturbation evolution at the inner face of a sufficiently thick cylindrical shell so that we can ignore the transference to this surface of the perturbations at the outer surface (feedthrough effects). However, in the case when $\rho_1 \ll \rho_2$ [$A_T = (\rho_2 - \rho_1)/(\rho_2 + \rho_1) = 1$, where A_T is the Atwood number], which is a convenient extreme case for studying the convergence effects, the value of α_1 becomes irrelevant.

On the other hand, for studying the perturbation evolution at the outer face of a shell imploded by an external pressure p_e , it is more suitable to consider the opposite extreme case $\rho_1 \gg \rho_2$ ($A_T = -1$) in which now α_2 becomes irrelevant, and to take $\alpha_1 = 0$ to describe the shell as incompressible. In this case, the assumption of a sink of mass at the interior region is more suitable because it allows the interior fluid to evolve meaningfully, as would be the case if it were a hollow shell [7]. It may be worthwhile to notice that in the present work, the values of the Atwood number $A_T = \pm 1$ refer to

the situations on the RTI stable internal surface and the RTI unstable external surface, respectively, of a thick shell.

2. $\rho_1 \ll \rho_2$

As we have just discussed, this case is the appropriate one for studying the perturbation growth at the internal surface of a thick shell. Then, Eq. (27) reads

$$\ddot{\xi} + (2 - \alpha_2)\dot{\xi}\frac{\dot{R}}{R} - (m + \alpha_2 - 1)\xi\frac{\ddot{R}}{R} = 0, \quad (28)$$

which can be reduced to the canonical form by the well-known transformation

$$\xi = \zeta \exp\left(-\frac{2 - \alpha_2}{2} \int_0^t \frac{\dot{R}}{R} dt\right) = \zeta \left(\frac{R_0}{R}\right)^{\frac{2 - \alpha_2}{2}}, \quad (29)$$

where $\zeta = \zeta(t)$ satisfies the following equation:

$$\ddot{y} = -\Omega^2 y, \quad \Omega^2 = \frac{2 - \alpha_2}{4} \frac{\dot{x}^2}{x^2} - \left(m + \frac{\alpha}{2}\right) \frac{\ddot{x}}{x}, \quad (30)$$

and the following dimensionless variables have been defined:

$$y = \frac{\zeta}{\zeta_0}, \quad \Omega = \frac{\omega}{\omega_0}, \quad (31)$$

and $\zeta_0 = \zeta(t=0)$ and $\omega_0 = \omega(t=0) = -(m + \alpha_2/2)(\dot{R}_0/R_0)$.

As is well known, an approximate solution of Eq. (27) can be obtained by using the WKB approximation, which yields

$$y = \sqrt{\frac{\Omega_0}{\Omega}} \cos\left(\int_0^T \Omega dT\right), \quad (32)$$

where we have taken $\dot{y}(0) = 0$, and

$$\Omega_0^2 = \frac{2(1 - \Pi_0)(2m + \alpha_2)}{(2 - \alpha_2)\ln(1 + a_0) + a_0\alpha_2}. \quad (33)$$

For writing the previous expression, we have used Eqs. (12) and (30). Then, the dimensionless perturbation amplitude turns out to be

$$z = yx^{-\frac{2 - \alpha_2}{2}}, \quad z = \frac{\xi}{\xi_0}. \quad (34)$$

We can see that the time evolution of the perturbation amplitude consists, in this case, of an oscillation with a maximum amplitude $Z(T)$, which constitutes the envelope of such an oscillation:

$$Z(T) = \sqrt{\frac{\Omega_0}{\Omega}} \frac{1}{x^{2 - \alpha_2}}. \quad (35)$$

In Fig. 3 we show $z(T) = \xi(t)/\xi_0$, which is obtained from solving Eq. (28) for the incompressible case ($\alpha_2 = 0$), for which the convergence effects are maximal, and for several different modes m . We have also represented the maximum amplitude $Z(T)$ of the perturbation oscillation, such as that given by the WKB approximation in Eq. (35), which quite accurately bounds the oscillation for every mode until the time close to the maximum velocity when the oscillation frequency is not yet too small to break the approximation. As was noticed by Book and Bodner [3], the amplitude in Eq. (32) decreases as $\Omega^{-1/2}$ as a consequence of the constancy of the action variable of the perturbation [3,7].

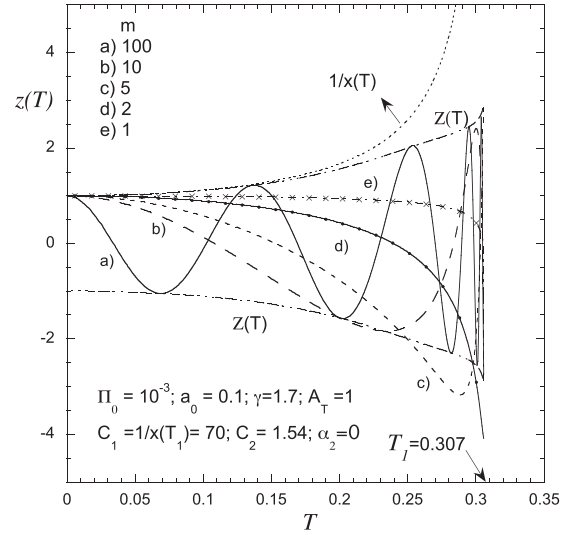


FIG. 3. Perturbation amplitudes $z(T) = \xi/\xi_0$ such as that given by Eq. (28) for different perturbation modes m . It is bounded by the envelope $Z(t)$ given by the WKB approximation in Eq. (35). A small-dotted line shows the $1/x$ perturbation growth due only to the geometrical effects.

A quite clear physical picture of this process can be extracted from the approach taken by Eliezer and Gray for solving the mathematical problem posed in Eq. (30) [45]. In fact, the one-dimensional motion in the coordinate $\zeta(T)$ can be seen as the projection of the two-dimensional motion of a particle under the attraction of a central force. The latter motion is governed by the following equations:

$$\ddot{\vec{u}} + \Omega^2 \vec{u} = 0, \quad (36)$$

where the vector \vec{u} has Cartesian components u_x and u_y , so that the previous vectorial equation can be written in the respective polar components ($u_x = u \cos \theta$, $u_y = u \sin \theta$, and $u = |\vec{u}|$) as follows:

$$\ddot{u} + u(\Omega^2 - \dot{\theta}^2) = 0, \quad (37)$$

$$\frac{1}{u} \frac{(u^2 \dot{\theta})}{dt} = 0. \quad (38)$$

For $\Omega^2 \gg \ddot{u}/u$, the previous equations yield $u \approx \dot{\theta}^{-1/2} \approx \Omega^{-1/2}$. That is, conservation of the angular momentum requires the reduction of the amplitude in Eq. (32) as the oscillation frequency increases, provided that Ω is not very small, which is the condition for the WKB approximation to remain valid. The good agreement with the exact solution of Eq. (28) indicates that this requirement is well satisfied during the imploding acceleration phase. Therefore, in such a phase, the convergence effects given by the term $x^{-(2 - \alpha_2)/2}$ in Eq. (35) are strongly mitigated by the conservation of the angular momentum, and the perturbation amplitude is not expected to increase much more than a factor of 2, as shown in Fig. 3. A similar conclusion was obtained in Ref. [3] for spherical geometry.

3. $\rho_1 \gg \rho_2$

This situation can be considered as a suitable description of the conditions present on the outer surface of a relatively thick shell. The assumption of incompressibility ($\alpha_1 = 0$) imposes the existence of a mass sink in the interior of the region “1.” Thus, from Eq. (27) the evolution of the perturbations is given now by the following equation:

$$\ddot{\xi} + (2 - \alpha_1)\xi\frac{\dot{R}}{R} + (m - \alpha_1 + 1)\xi\frac{\ddot{R}}{R} = 0. \quad (39)$$

Performing, as before, the transformation given by Eq. (29) but replacing α_2 with α_1 , we have now, instead of Eq. (30),

$$\ddot{y} = \sigma^2 y \quad \sigma^2 = \frac{2 - \alpha_1}{4} \frac{\dot{x}^2}{x^2} - \left(m - \frac{\alpha}{2}\right) \frac{\ddot{x}}{x}, \quad (40)$$

and the approximate WKB solution reads

$$z = \frac{\xi}{\xi_0} = \sqrt{\frac{\sigma_0}{\sigma}} \frac{1}{x^{2-\alpha_1}} \cosh\left(\int_0^T \sigma dT\right), \quad (41)$$

where we have imposed the initial condition $\dot{z}_0 = 0$, and σ_0 is defined as follows:

$$\sigma_0^2 = \frac{4(1 - \Pi_0)(2m + \alpha_1)}{(2 - \alpha_1)\ln(1 + a_0) + a_0\alpha_1}. \quad (42)$$

In this case, the interface is RT-unstable and the geometrical effects act to enhance the perturbation growth, which turns out to be the maximum for the incompressible case ($\alpha_1 = 0$). Nevertheless, for relatively thick shells, like in the case of LAPLAS, the convergence ratio of the external surface is not very large, and the geometrical effects are not expected to be considerable. In fact, as we have previously discussed, for LAPLAS such a convergence ratio is less than 1.5, and although the shell is practically incompressible, the perturbation growth is mainly due to RTI on a practically planar surface, and it can only be mitigated or suppressed by the mechanical (nonideal) properties of the shell material.

C. Elastic media

As we have already mentioned, in the LAPLAS experimental setup, the stability of the cylindrical implosion is envisaged to be controlled by means of the elastic-plastic properties of the shell media. Since the stability in the elastic regime is a necessary condition for the stability of the interface [32,38], we will consider here the influence of the elastic properties of the shell on the perturbation growth in the presence of the convergence effects.

In the irrotational approximation, the boundary condition in Eq. (21) must be modified in such a manner that now the continuity of the normal stress reads

$$-\delta p_1(R) + S_{rr}^{(1)} = -\delta p_2(R) + S_{rr}^{(2)}, \quad (43)$$

where $S_{rr}^{(n)}$ are the normal component of the perturbations $\delta r_{ik}^{d(n)}$ of the deviatoric part $t_{ik}^{d(n)}$ of the stress tensor $t_{ik}^{(n)}$ ($t_{ik}^{(n)} = -p_n \delta_{ik} + t_{ik}^{d(n)}$ and $\delta t_{ik}^{d(n)} \equiv S_{ik}^{(n)}$). The deviatoric part is determined by the constitutive properties of the medium, and, for the case of elastic media, they are given by the Hooke law. Then, for elastic media, we have

$$\dot{S}_{rr}^{(n)} = 2G_n \frac{\partial(\delta v_n)}{\partial r} \Big|_r = R, \quad (44)$$

where G_n is the shear modulus of the medium n . Thus, from Eqs. (23)–(26) we obtain the following expressions:

$$\dot{S}_{rr}^{(1)} = 2G_1(m-1) \frac{\dot{\xi}R - (\alpha_1 - 1)\xi\dot{R}}{R^2}, \quad (45)$$

$$\dot{S}_{rr}^{(2)} = -2G_2(m+1) \frac{\dot{\xi}R - (\alpha_2 - 1)\xi\dot{R}}{R^2}, \quad (46)$$

and the equation for the perturbations evolution becomes

$$\begin{aligned} \ddot{\xi} + \frac{(2 - \alpha_2)\rho_2 + (2 - \alpha_1)\rho_1}{\rho_2 + \rho_1} \xi \frac{\dot{R}}{R} \\ - \frac{(m + \alpha_2 - 1)\rho_2 - (m - \alpha_1 + 1)\rho_1}{\rho_2 + \rho_1} \xi \frac{\ddot{R}}{R} \\ = \frac{m}{(\rho_2 + \rho_1)R} (S_{rr}^{(1)} - S_{rr}^{(2)}). \end{aligned} \quad (47)$$

In order to get a solution to this equation, we must integrate it together with Eqs. (45) and (46). Now, the use of the WKB approximation is not feasible, and it must be solved numerically.

As for the case of ideal media, we will consider separately the cases with $\rho_1 \ll \rho_2$ and $\rho_1 \gg \rho_2$, suitable for describing the amplitude evolution in the inner and outer surfaces of a thick shell, respectively.

1. $\rho_1 \ll \rho_2$

From Eq. (47) and using dimensionless magnitudes as defined in Eqs. (11) and (34), we obtain

$$\ddot{z} + (2 - \alpha_2)z\frac{\dot{x}}{x} - z\frac{\ddot{x}}{x}(m - 1 + \alpha_2) = mB_{e2}\frac{S_2}{x}, \quad (48)$$

$$\dot{S}_2 = 2(m+1) \frac{[\dot{z}x - (\alpha_2 - 1)z\dot{x}]}{x^2}, \quad (49)$$

where

$$\dot{S}_2 = \frac{\dot{S}_{rr}^{(2)}}{S_{0e}}, \quad \dot{S}_{0e} = G_2 \frac{\xi_0}{R_0}, \quad B_{e2} = \frac{G_2}{p_e}. \quad (50)$$

These equations must be solved with the following initial conditions:

$$x(0) = z(0) = 1, \quad \dot{x}(0) = \dot{z}(0) = 0. \quad (51)$$

We show in Figs. 4(a) and 4(b) the perturbation evolution for two typical low ($m = 5$) and high ($m = 100$) modes, respectively, for the incompressible case ($\alpha_2 = 0$), and for different values of the parameter B_{e2} that measures the influence of the medium “2” elasticity. As is expected, for $B_{e2} = 0$ we retrieve the ideal case previously considered in which the perturbation growth due to the geometrical effects was only limited by the conservation of the angular momentum. For relatively small values of B_{e2} ($B_{e2} = 0.01$), the elasticity produces a further damping that progressively vanishes as B_{e2} increases, and for a sufficiently large value of B_{e2} the elasticity finally destroys the favorable effects of the angular momentum conservation. In fact, for very large values of B_{e2} , the effects of the elasticity completely dominate in Eq. (48), so that from Eq. (49) we have

$$\dot{z}x \approx (\alpha_2 - 1)z\dot{x} \quad \text{or} \quad z \approx x^{-(1-\alpha_2)}. \quad (52)$$

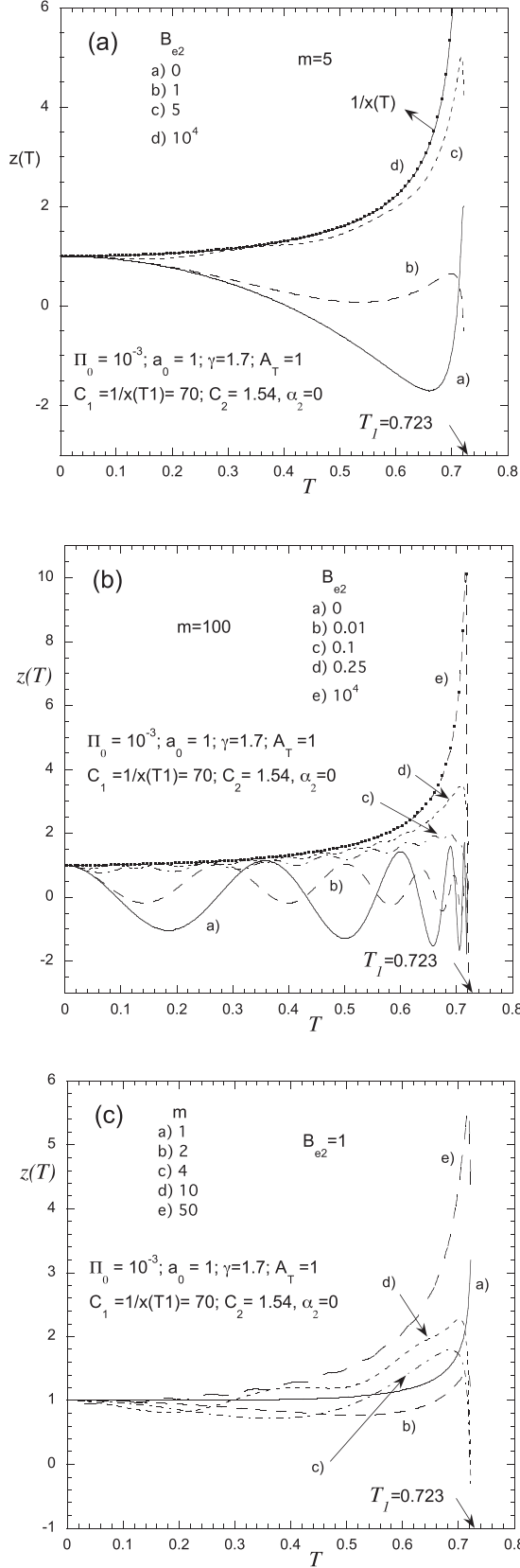


FIG. 4. Time evolution of the dimensionless perturbation amplitude $z(t)$ for different values of the parameter B_{e2} and different modes m . (a) $m = 5$; (b) $m = 100$; (c) $B_{e2} = 1$.

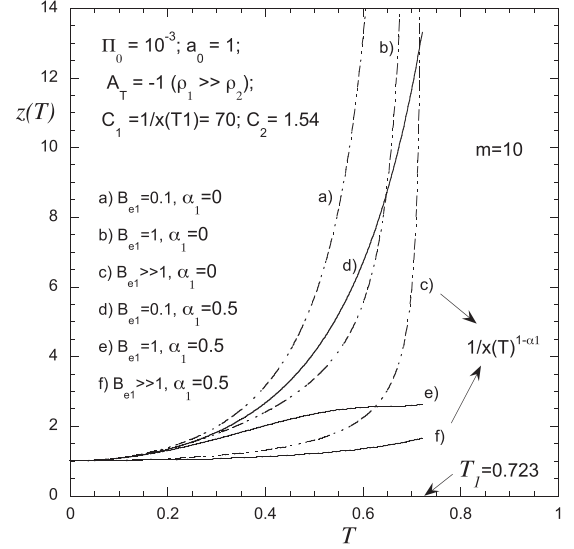


FIG. 5. Perturbation amplitude $z(T)$ for different values of the parameter B_{e1} and for two values of the compressibility factor α_1 .

That is, in this limit the geometrical effects completely dominate without any damping by the angular momentum conservation, as observed in the ideal case. This is because of the suppression by the elasticity of such an effect, so that the perturbation growth is only mitigated by the compressibility of the medium. Certainly such a mitigation due the compressibility becomes significant when $\alpha_2 \sim 1$ or larger, a situation that in LAPLAS could only be eventually present during the stagnation phase when the pusher would be more compressible. In such a case, it would further reduce the BP effect during the stagnation phase, thus reinforcing the expectation that the perturbation growth during such a phase is mainly controlled by the RTI without too much influence of the convergence.

In Fig. 4(c) we show the perturbation evolution for $B_{e2} = 1$, which would be the typical case for the LAPLAS experiments. We can see that only the very large modes show some considerable perturbation growth. Such modes, however, are expected to have the smallest amplitudes [46], so that more growth could be tolerated.

2. $\rho_1 \gg \rho_2$

In this case, we assume that a sink of mass exists in the interior of medium “1” that makes possible an arbitrary variation of the density ρ_1 as determined by a given value of α_1 [6,7]. Then, Eq. (47) in dimensionless magnitudes now reads

$$\ddot{z} + (2 - \alpha_1)\dot{z}\frac{\dot{x}}{x} - + z\frac{\ddot{x}}{x}(m + 1 - \alpha_1) = mB_{e1}\frac{\dot{S}_1}{x}, \quad (53)$$

$$\dot{S}_1 = 2(m - 1)\frac{[\dot{z}x - (\alpha_1 - 1)z\dot{x}]}{x^2}, \quad (54)$$

where

$$\dot{S}_1 = \frac{\dot{S}_{rr}^{(1)}}{\dot{S}_{0e}}, \quad \dot{S}_{0e} = G_1 \frac{\xi_0}{R_0}, \quad B_{e1} = \frac{G_1}{p_e}. \quad (55)$$

As in the previous paragraph, for $B_{e1} = 0$ we retrieve the ideal case that is dominated by the RTI and the BP convergence

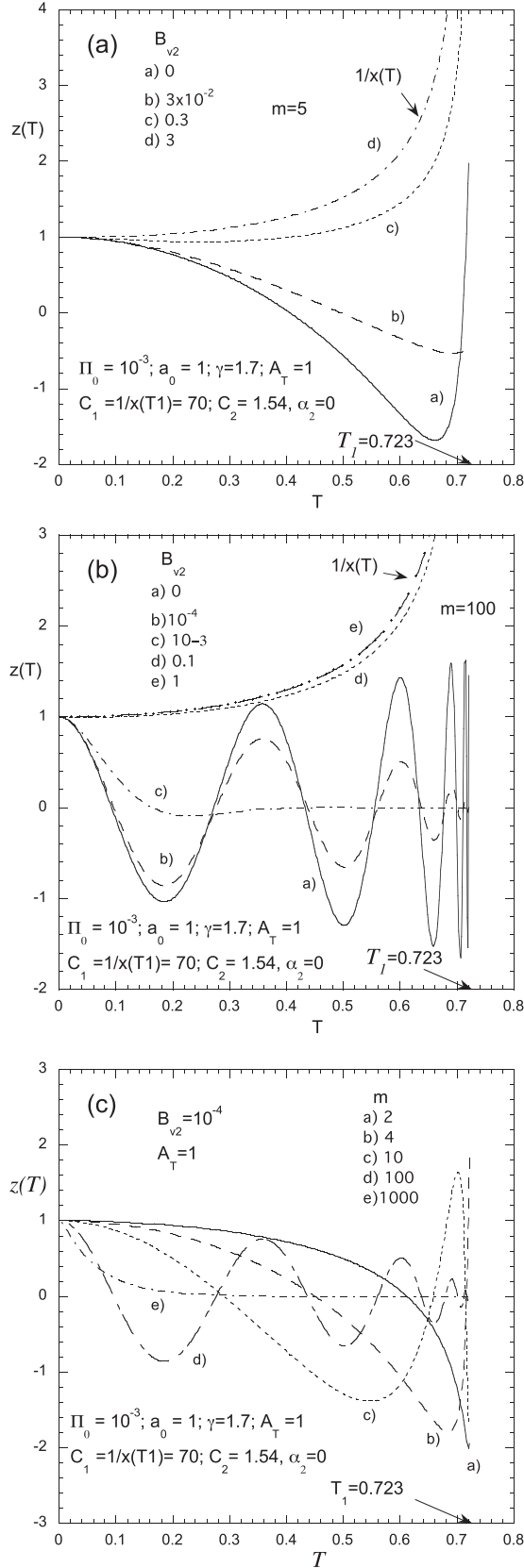


FIG. 6. Time evolution of the dimensionless perturbation amplitude $z(t)$ for different values of the parameter B_{e2} and different modes m . (a) $m = 5$; (b) $m = 100$; (c) $B_{v2} = 10^{-4}$.

effects. As B_{e1} increases, the elasticity first mitigates the growth due to RTI as it does in the case of a static (in average) interface, but with no direct effect on the growth due to the geometrical convergence. However, it shows an indirect effect that is clearly seen when elasticity completely dominates for very large values of B_{e1} for which it becomes $S_1 \ll 1$:

$$z \approx x^{-(1-\alpha_1)}. \quad (56)$$

As can be noticed, the presence of the elasticity enhances the sensitivity of the compressibility of the medium on the convergence effects in comparison with the ideal case:

$$z \approx x^{-\left(\frac{2-\alpha_1}{2}\right)}. \quad (57)$$

It is interesting to notice that under a strong influence of the elasticity, the geometrical convergence effects manifest themselves in a manner that is different from the already known BP convergence effect occurring in ideal media. In addition, as shown by Eqs. (52) and (56), this mechanism works equally well in both situations, either when the interface is RT-unstable or RT-stable. As we have seen, in the second case it destroys the beneficial effects of the angular momentum conservation.

Furthermore, even in the case when the elasticity would be able to stabilize RTI, it will only affect the growth due to the geometrical BP effects provided that the compressibility of the denser medium plays a significant role. This will not be the case of LAPLAS, and the convergence will be fully in effect at the maximum rate. Nevertheless, since the convergence ratio of the external surface of the LAPLAS is actually very low ($C_e = C_1 C_2 \leq 1.5$) [16–18,27], the results of the planar analysis of RTI would not be considerably affected by the geometrical convergence.

We show an example of the behavior above discussed in Fig. 5 for $\alpha_1 = 0$ and 0.5, and different values of the parameter B_{e1} . For each value of α_1 the perturbation grows, in general, due to both RTI and convergence. But, for the largest values of B_{e1} , RTI becomes stabilized, and the perturbation grows as $x^{-(1-\alpha_1)}$ only due to the geometrical convergence and mitigated by the presence of the compressibility.

D. Viscous media

As we have already mentioned, the influence of viscosity on the perturbation growth in the presence of BP geometrical effects was considered in Ref. [11] for the case of the expansion of a cylindrical cavity. But since the background motion was not included in the equations, the consequences of the viscosity were not completely studied. Here, we can briefly consider such consequences by using Eq. (47) with $S_{rr}^{(n)}$ given now by the following expressions corresponding to Newtonian fluids:

$$S_{rr}^{(1)} = 2\mu_1(m-1) \frac{\xi \dot{R} - (\alpha_1 - 1)\xi \dot{R}}{R^2}, \quad (58)$$

$$S_{rr}^{(2)} = -2\mu_2(m+1) \frac{\xi \dot{R} - (\alpha_2 - 1)\xi \dot{R}}{R^2}, \quad (59)$$

where μ_n is the dynamic viscosity of the medium “ n .”

When $\rho_1 \ll \rho_2$ ($A_T = 1$), Eqs. (44) and (59) yield the following evolution equation for the perturbation amplitude

in dimensionless form:

$$\begin{aligned} \ddot{z} + (2 - \alpha_2)z\frac{\dot{x}}{x} - z\frac{\ddot{x}}{x}(m - 1 + \alpha_2) \\ = 2B_{v2}m(m + 1)\frac{[\dot{z}x - (\alpha_2 - 1)z\dot{x}]}{x^3}, \end{aligned} \quad (60)$$

where

$$B_{v2} = \frac{\mu_2}{\rho_2 R_0} \sqrt{\frac{\rho_2}{p_e}}. \quad (61)$$

As for the elastic case, this situation is appropriate for describing the inner surface of a thick shell. In Figs. 6(a) and 6(b), we show the perturbation evolution when the heavy medium is incompressible ($\alpha_2 = 0$), and for $m = 5$ and 100, respectively, as representatives of the behavior for low and high modes. As we have already noticed, when $B_{v2} = 0$ we have the ideal medium situation in which the perturbations are strongly reduced by the angular momentum conservation. When the effect of the viscosity becomes relevant, it provides some damping to the growth of the perturbations provided that B_{v2} is not too large (for instance, for $B_{v2} \leq 0.1$). But, as in the elastic case, as soon as the viscosity becomes large enough, it reduces the surface waves oscillation frequency and destroys the damping effect of the angular momentum conservation ($B_{v2} = 1$ and 3). This is probably a rather unrealistic physical situation because such high values of the B_{v2} parameter are not likely to be achieved in practice. But it illustrates how the dominance of the viscosity in Eq. (60) gives rise to a manifestation of the geometrical convergence effect, which is different from the well-known BP effect, and that is only affected by the compressibility of the medium, just as was shown for the elastic case in Eq. (56).

In Fig. 6(c) we show the perturbation evolution for $B_{v2} = 10^{-4}$ for a wide range of values of the modes m . Such a value of B_{v2} is the typical one in the experiment of Ref. [11], and we can see that it is very effective for damping practically all the modes m .

For the limit $\rho_1 \gg \rho_2$, the general conclusions are qualitatively similar to those for the elastic case. Of course, viscosity cannot completely stabilize RTI as elasticity does, but it can provide some growth damping of the RTI. Nevertheless, it will also be unable to affect the growth of the perturbations due to the geometrical convergence, unless a significant compressibility of the media is present, such as is reflected in Eq. (56).

III. CONCLUDING REMARKS

We have analyzed the influence of the mechanical properties (elasticity and viscosity) of the two media involved in the inward acceleration phase of a cylindrical implosion on the RT-stable and unstable configurations.

In the RT-stable configuration occurring at the inner face of a thick shell, the rapid increase of the oscillation frequency

during the implosion effectively damps the growth of the perturbations due to the geometrical convergence, thanks to the angular momentum conservation, when media at both sides of the interface are ideal.

When the media have elastic properties, the angular momentum conservation process remains still active for moderate values of the dimensionless elastic shear modulus B_{e2} of the material. But for relatively high values of B_{e2} , the elastic properties reduce the oscillation frequency and destroy the damping effect of the angular momentum conservation. In this limit, geometrical convergence dominates the perturbation growth, although it acts in a somewhat different manner compared with the ideal case, making the process more sensitive to the material compressibility than in the ideal case. This mechanism also works in the unstable configuration occurring at the outer face of the thick shell, in such a manner that, once again, for moderate values of the dimensionless elastic shear modulus B_{e1} , the elasticity is able to stabilize RTI but without affecting the growth of the perturbations due to the geometrical convergence, except for the fact that elasticity makes the compressibility of the media more effective than in the case involving ideal media in reducing the perturbation growth.

A qualitatively similar behavior is observed when the media are viscous, with the difference, of course, that viscosity is unable to completely stabilize RTI in the external surface of the shell.

Regarding the application to the LAPLAS experimental setup, the low convergence ratio of the external surface makes the convergence effects practically nonoperational, and therefore the surface can be treated as reasonably planar for the analysis of the RTI. On the other hand, at the internal surface, the typical value of $B_{e2} \sim 1$ in LAPLAS is still sufficiently low as to not completely destroy the process of damping due to the angular momentum conservation, so that the perturbation growth due to the geometrical convergence remains reasonably low even in the incompressible limit.

For applications to cylindrical implosions of liners driven by intense electrical currents, the effects of the viscosity combined with the liner compressibility may positively influence the perturbation growth as it makes the compressibility more effective than in the absence of viscosity for moderating the growth of the perturbations due to the geometrical convergence.

ACKNOWLEDGMENTS

This work has been partially supported by the Ministerio de Economía y Competitividad of Spain (Grant No. PID2021-125550OB-I00), and by the BMBF of Germany.

- [1] G. I. Bell, Los Alamos National Laboratory, Report LA-1321 (1951) (unpublished). Available at <https://sgp.fas.org/othergov/doe/lanl/lib-www/la-pubs/00356818.html>.
 [2] M. S. Plesset, *J. Appl. Phys.* **25**, 96 (1954).

- [3] D. L. Book and S. E. Bodner, *Phys. Fluids* **30**, 367 (1987).
 [4] V. N. Goncharov, P. McKenty, S. Skupsky, R. Betti, R. L. McCrory, and C. Cherfils-Clérouin, *Phys. Plasmas* **7**, 5118 (2000).

- [5] P. Amendt, J. D. Colvin, J. D. Ramshaw, H. F. Robey, and O. L. Landen, *Phys. Plasmas* **10**, 820 (2003).
- [6] J. D. Ramshaw and P. A. Amendt, *Phys. Rev. E* **67**, 056304 (2003).
- [7] R. Epstein, *Phys. Plasmas* **11**, 5114 (2004).
- [8] A. L. Velikovich and P. F. Schmit, *Phys. Plasmas* **22**, 122711 (2015).
- [9] Y. Zhou, *Phys. Rep.* **720-722**, 1 (2017).
- [10] Y. Zhou, R. J. R. Williams, P. Ramaprabhu, M. Groom, B. Thornber, A. Hillier, W. Mostert, B. Rollin, S. Balachandar, P. D. Powell, A. Mahalov, and N. Attal, *Physica D* **423**, 132838 (2021).
- [11] Z. Wang, K. Xue, and P. Han, *Phys. Fluids* **33**, 034118 (2021).
- [12] G. Terrones and M. D. Carrara, *Phys. Fluids* **27**, 054105 (2015).
- [13] G. Terrones and T. Heberling, *Phys. Fluids* **32**, 094105 (2020).
- [14] Y. B. Sun, R. H. Zeng, and J. J. Tao, *Phys. Plasmas* **28**, 062701 (2021).
- [15] A. R. Piriz, S. A. Piriz, and N. A. Tahir, *Phys. Rev. E* **104**, 035102 (2021).
- [16] N. A. Tahir, D. H. H. Hoffmann, J. A. Maruhn, P. Spiller, and R. Bock, *Phys. Rev. E* **60**, 4715 (1999).
- [17] N. A. Tahir, V. Kim, A. Matvechev, A. Ostriker, A. V. Shutov, I. V. Lomonosov, A. R. Piriz, J. J. López Cela, and D. H. H. Hoffmann, *Nucl. Instrum. Methods Phys. Res., Sect. B* **245**, 85 (2006).
- [18] N. A. Tahir, A. Shutov, I. V. Lomonosov, A. R. Piriz, D. H. H. Hoffmann, C. Deutsch, and V. E. Fortov, *Phys. Rev. E* **79**, 046410 (2009).
- [19] N. A. Tahir, I. V. Lomonosov, B. Borm, A. R. Piriz, P. Neumayer, A. Shutov, V. Bagnoud, and S. A. Piriz, *Contrib. Plasma Phys.* **57**, 493 (2017).
- [20] N. A. Tahir, P. Neumayer, I. V. Lomonosov, A. Shutov, V. Bagnoud, A. R. Piriz, S. A. Piriz, and C. Deutsch, *Phys. Rev. E* **101**, 023202 (2020).
- [21] N. A. Tahir, I. V. Lomonosov, B. Borm, A. R. Piriz, A. Shutov, P. Neumayer, V. Bagnoud, and S. A. Piriz, *Astrophys. J. Suppl. Ser.* **232**, 1 (2017).
- [22] N. A. Tahir, A. Shutov, I. V. Lomonosov, A. R. Piriz, P. Neumayer, V. Bagnoud, and S. A. Piriz, *Astrophys. J. Suppl.* **238**, 27 (2018).
- [23] N. A. Tahir, P. Neumayer, A. Shutov, A. R. Piriz, I. V. Lomonosov, V. Bagnoud, S. A. Piriz, and C. Deutsch, *Contrib. Plasma Phys.* **59**, e201800143 (2019).
- [24] N. A. Tahir, A. Shutov, A. R. Piriz, P. Neumayer, I. V. Lomonosov, V. Bagnoud, and S. A. Piriz, *Contrib. Plasma Phys.* **59**, e201800135 (2019).
- [25] N. A. Tahir, A. Shutov, P. Neumayer, V. Bagnoud, A. R. Piriz, I. V. Lomonosov, and S. A. Piriz, *Phys. Plasmas* **28**, 032712 (2021).
- [26] N. A. Tahir, H. Juránek, A. Shutov, R. Redmer, A. R. Piriz, M. Temporal, D. Varentsov, S. Udrea, D. H. H. Hoffmann, C. Deutsch, I. Lomonosov, and V. E. Fortov, *Phys. Rev. B* **67**, 184101 (2003).
- [27] A. R. Piriz, R. F. Portugues, N. A. Tahir, and D. H. H. Hoffmann, *Phys. Rev. E* **66**, 056403 (2002).
- [28] N. A. Tahir, B. Goddard, V. Kain, R. Schmidt, A. Shutov, I. V. Lomonosov, A. R. Piriz, M. Temporal, D. H. H. Hoffmann, and V. E. Fortov, *J. Appl. Phys.* **97**, 083532 (2005).
- [29] G. Terrones, *Phys. Rev. E* **71**, 036306 (2005).
- [30] G. Terrones, *J. Appl. Phys.* **102**, 034908 (2007).
- [31] A. R. Piriz, J. J. López Cela, N. A. Tahir, and D. H. H. Hoffmann, *Phys. Rev. E* **78**, 056401 (2008).
- [32] A. R. Piriz, J. J. López Cela, and N. A. Tahir, *Phys. Rev. E* **80**, 046305 (2009).
- [33] S. A. Piriz, A. R. Piriz, and N. A. Tahir, *Phys. Rev. E* **95**, 053108 (2017).
- [34] S. A. Piriz, A. R. Piriz, and N. A. Tahir, *Phys. Rev. E* **96**, 063115 (2017).
- [35] S. A. Piriz, A. R. Piriz, and N. A. Tahir, *Phys. Rev. E* **97**, 043106 (2018).
- [36] S. A. Piriz, A. R. Piriz, and N. A. Tahir, *J. Fluid Mech.* **867**, 1012 (2019).
- [37] S. A. Piriz, A. R. Piriz, and N. A. Tahir, *Phys. Fluids* **30**, 111703 (2018).
- [38] A. R. Piriz, S. A. Piriz, and N. A. Tahir, *Phys. Rev. E* **100**, 063104 (2019).
- [39] S. A. Piriz, A. R. Piriz, N. A. Tahir, S. Richter, and M. Bestehorn, *Phys. Rev. E* **103**, 023105 (2021).
- [40] J. J. López Cela, A. R. Piriz, M. C. Serna Moreno, N. A. Tahir, and D. H. H. Hoffmann, *Laser Part. Beams* **24**, 427 (2006).
- [41] T. G. Leighton, *The Acoustic Bubble* (Academic, London, 1997), p. 303.
- [42] Y. A. Ilinskii, E. A. Zabolotskaya, T. A. Hay, and M. F. Hamilton, *J. Acoust. Soc. Am.* **132**, 1346 (2012).
- [43] S. Sugimoto and Y. W. Kwon, Multiscale and Multidisciplinary Modeling, *Exp. Design* **3**, 295 (2020).
- [44] S. Chandrasekhar, *Q. J. Mech. Appl. Math.* **8**, 1 (1955).
- [45] C. J. Eliezer and A. Gray, *SIAM J. Appl. Math.* **30**, 463 (1976).
- [46] A. Bret, A. R. Piriz, and N. A. Tahir, *Phys. Rev. E* **85**, 036402 (2012).